

**©1999 IEEE. Personal use of this material is permitted. However, permission to reprint/republish this material for advertising or promotional purposes or for creating new collective works for resale or redistribution to servers or lists, or to reuse any copyrighted component of this work in other works must be obtained from the IEEE.**

## Measurement of the Energy Sensitivity of a Superconductive Comparator

David A. Feld, Jay P. Sage, Karl K. Berggren, and Aleem Siddiqui

Lincoln Laboratory, Massachusetts Institute of Technology, Lexington, MA 02420-9185, USA

**Abstract**—Comparators are a critical component in sigma-delta A/D converters. We have studied experimentally the sensitivity of a quantum flux parametron (QFP) comparator operated over a range of sampling frequencies  $F_S$  from 40 Hz to 40 MHz. In one experimental method, following Ko and Lee, we measure the firing probability of the QFP as a function of applied flux. The sensitivity can be derived from the slope of this curve. In a second method, we measure the sensitivity directly by observing the spectrum of the QFP output while the amplitude of a small sinusoidal applied flux is adjusted to exceed the noise floor by 3 dB. The two methods were found to be in good, but not perfect agreement. The sensitivity was measured as we varied both  $F_S$  and the clock rise time. The spectrum of the quantization noise exhibits, as expected, a flat floor whose level is inversely proportional to  $F_S$ . The best energy sensitivity that we observed was for a clock frequency of  $\sim 20$  MHz with a 10 ns rise time. The measured sensitivity was about  $1500 h$  (Planck's constant). The readout circuit prevented us from clocking the comparator into the GHz range for even greater sensitivity. We also believe that the comparator could be optimized to improve sensitivity further. The noise floor was low enough that we could observe excess low-frequency noise below 5 Hz. We have not yet determined whether it is intrinsic to the comparator or originates from our test electronics. We hypothesize that the noise floor will continue to fall as  $F_S$  increases until we reach the speed limit of the comparator, at which point successive output samples will no longer be uncorrelated, or until we reach the uncertainty-principle limit ( $h$ ) in the 100s of GHz range.

### I. INTRODUCTION

Analog comparators are used in the front-ends of high-resolution A/D converters [1,2,3], timing discriminators, and other analog circuits. To properly characterize the behavior of these analog front-ends operating at GHz clock frequencies it is imperative that the comparators they comprise be fully characterized. One important figure of merit for a comparator is its energy sensitivity  $S_E$ , which is of fundamental importance and which to the best of our knowledge has not yet been studied. In this paper we describe an experimental procedure to measure the energy sensitivity of a comparator and to compare it with the theoretical sensitivity of an ideal comparator.

We operate a quantum flux parametron (QFP) comparator in an open-loop configuration (without feedback) to measure the power spectral density of its output. We clock the QFP at sampling frequencies  $F_S$  from 40 Hz to 40 MHz, and we observe that the white noise floor power is inversely proportional to the frequency of operation as is expected. Further-

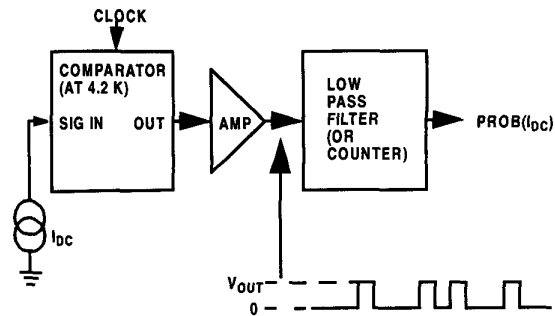


Fig. 1. Experimental setup to measure gray zone of comparator. A dc input is applied to the input of a superconductive comparator under test. The data (1s and 0s) are amplified and read out to room temperature where they are low pass filtered. The output voltage can be converted to a probability that the output is a "1".

more, we measure the energy sensitivity to be approximately  $1500 h$  (Planck's constant) at  $F_S = 20$  MHz with a clock rise time of 10 ns. This sensitivity is found to be in good but not perfect agreement with theory. We also observe that the low-frequency excess noise floor intercepts the white noise floor at below 5 Hz. Our measurement technique remains applicable above 1 GHz, where some analog front-ends are now operated. For 10s of GHz operation, it may be difficult to measure the noise floor of a comparator, and experiments that measure the correlation between adjacent output samples may be used to determine the highest frequency at which a comparator can be clocked and still exhibit ideal behavior. We suggest that our experimental techniques be applied to QFP, rapid single flux quantum (RSFQ), and other comparators when clocked at GHz frequencies to better characterize these basic circuit elements.

#### A. Measurement and Theory of the "Gray" Zone

Previous work on comparators has centered around the measurement of the "gray" zone using the type of experiment illustrated in Fig. 1. The input is fixed at a dc current level while the comparator is repeatedly clocked. The digital output state of the comparator is detected by room temperature electronics. The fraction of clock cycles in which the comparator generates a "1" is recorded as a probability. The experiment is repeated for a range of dc input currents, and the results are plotted. Fig. 2 shows a typical experimental plot of the gray zone, in this case for a QFP comparator. The width of the gray zone is determined by the intrinsic thermal noise in the comparator and by the comparator's dynamics.

In the case of an RSFQ comparator, a "1" generates a tiny flux-quantum-sized output pulse, which does not have suffi-

Manuscript received September 15, 1998.

This work was supported by the Department of Defense through the Air Force Research Laboratory under Air Force Contract F19628-95-C-0002.

cient energy to be detected at room temperature. If the comparator is operated at GHz clock frequencies, then these tiny output pulses can be averaged on chip, and the fraction of the time that the output is a "1" can be measured as a dc voltage. This voltage can be recorded as a function of the dc input current, and it can be converted into a probability plot like that of Fig. 2.

Investigators have studied the shape of the gray zone with respect to circuit parameter values, temperature, shape of the comparator excitation pulse, etc., and there has been good agreement between measurements and theory [4,5,6]. However, the gray zone measurement is only an average measurement of the output data, and it does not measure the spectral distribution, which is of critical importance in many applications.

### B. Spectral Studies in Digital SQUID Magnetometers

A large body of work has gone into measuring the energy sensitivity of digital SQUID magnetometers. In some magnetometer designs the input signal is fed into a SQUID amplification stage before it is delivered into the input of a comparator [7]. In other designs, the input signal is directly connected to the input of a comparator [8,9,10]. In each of these designs, the comparator is placed in a feedback loop that allows the magnetometer to have a large dynamic range. This feedback band-limits the output spectrum to KHz or MHz frequencies, and it prohibits the observation of the high-frequency components in the comparator's output. We propose that a comparator be clocked at GHz speeds in an open-loop configuration (without any feedback), so that the entire output noise spectrum can be observed into the GHz range.

## II. ENERGY SENSITIVITY MEASUREMENT AND THEORY

### A. Previous Derivation of Energy Sensitivity

Ko and Lee [6] have derived expressions for the energy sensitivity of a QFP comparator following Fujimaki's work [11],

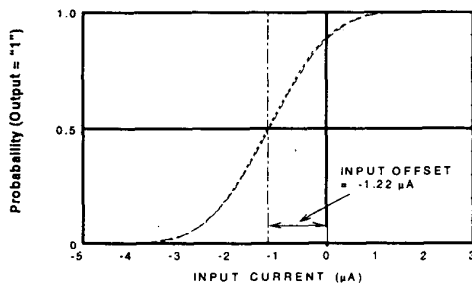


Fig. 2. Measurement of gray zone of quantum flux parametron.

which assumes that each output sample is independent of its neighbors. For a QFP biased in the gray zone they computed the energy sensitivity to be

$$S_{\epsilon} = \frac{2P_0(1-P_0)L}{\left(\frac{dP}{dI}\right)^2 f_B} \quad (1)$$

where  $P_0$  is the probability that the comparator's output is a "1",  $(1-P_0)$  is the probability that the output is a "0",  $L$  is the differential input inductance of the comparator,  $f_B$  is the clock frequency, and  $dP/dI$  is the slope of the gray zone curve at the point where the comparator is dc biased. Ko and Lee made measurements of  $dP/dI$  as a function of the slew rate of the clock, and from eq. (1) they could predict what the energy sensitivity should be at different operating frequencies. They did not, however, make sensitivity measurements. They calculated that it should be possible to approach uncertainty-principle-limited operation (a few h) if the QFP is operated near its bandwidth limit in the 10s of GHz. However, these calculations assume that: (1) there is no correlation between successive samples and (2) the comparator is sufficiently well isolated from extraneous signals in its environment that it is sensitive only to signals applied to its input. These assumptions must be tested.

### B. Alternative Derivation of Energy Sensitivity

We derive an alternate expression for energy sensitivity by measuring the amplitude of the minimum detectable sinusoidal input current. If this value is in agreement with the expression based on the slope,  $dP/dI$ , of the gray zone from eq. (1), then the assumption that the spectral density is white (no correlation between samples) is confirmed.

Derivation of the alternate expression follows. Suppose that we perform the experiment shown in Fig. 1, but this time we add a small ac waveform to the dc bias, as shown in Fig. 3. The input sinewave modulates the probability that the output will generate a "1" as follows:

$$P_{OUT}(t) = P_0 + \Delta P \sin(\omega_0 t) \quad (2)$$

If we assume that the output of the comparator is a sequence of impulses each of which has a probability  $P_{OUT}(t)$  of being a "1", then we can write an expression for the autocorrelation function of this modulated pulse train. The power spectral density, which is the Fourier transform of this autocorrelation function, is given by

$$S(\omega) = 2f_B \left[ P_0(1-P_0) - \frac{\Delta P^2}{2} \right] + \frac{f_B \Delta P^2}{2} \delta(\omega - \omega_0) \quad (3)$$

When the modulating probability  $\Delta P \ll 1$ , then eq. (3) can be approximated as

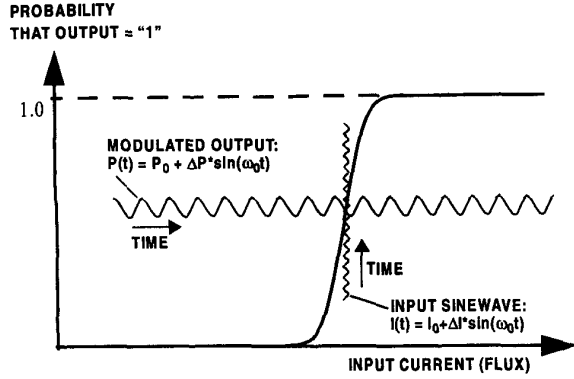


Fig. 3. Small sinewave added to the dc bias at the input of the comparator. Output probability is sinusoidally modulated.

$$S(\omega) = 2f_B[P_0(1-P_0)] + \frac{f_B^2 \Delta P^2}{2} \delta(\omega - \omega_0) \quad (4)$$

The left hand term of this equation is the quantization noise power of the output of the comparator as it samples its own thermal noise. The right side of the equation is the power in the output of the comparator due to the modulating (input) sinewave. Suppose that we integrate the white noise power [the left hand term of eq. (4)] over the interval  $[\omega_0 - \Delta B/2, \omega_0 + \Delta B/2]$ . The minimum detectable modulating sinewave can be defined as the minimum  $\Delta P$  required to make the integrated noise power in this interval equal to the output power associated with the modulating signal. Experimentally, these quantities will be equal when the power in this interval of width  $\Delta B$  is 3 dB larger than the magnitude in adjacent intervals of width  $\Delta B$  (where no modulating signal is present). This factor of 3 dB results from the fact that the white noise and the sine-wave add incoherently, so that their magnitude is equal when the noise floor in that bin is raised by 3 dB. So, the minimal detectable signal occurs when the power in the left hand term of eq. (4) integrated over a bandwidth  $\Delta B$  is equal to the power on the right hand term:

$$2f_B P_0(1-P_0)\Delta B = \frac{f_B^2 (\Delta P_{3dB})^2}{2} \quad (5)$$

For a comparator with a gray-zone slope  $dP/dI$ , we note that

$$I_{3dB} = \frac{\Delta P_{3dB}}{\frac{dP}{dI}} \quad (6)$$

By substitution of eq. (6) into eq. (5) and by multiplying both sides by the comparator's differential input inductance  $L$ , we get

$$S_\epsilon = \Delta E \Delta T = \left[ \frac{L(I_{3dB})^2}{2} \right] \frac{1}{\Delta B} = \frac{2P_0(1-P_0)L}{\left( \frac{dP}{dI} \right)^2 f_B} \quad (7)$$

Note that we have rearranged the terms so that the right hand side of eq. (7) fits the definition of energy sensitivity  $S_\epsilon$  given by the previous authors in eq. (1). In the next subsection we will show how the left hand side of this equation can be used to measure the energy sensitivity of the comparator.

### C. Proposed Energy Sensitivity Measurement Using the FFT

Advances in semiconductor test electronics make it possible to record lengthy waveforms from the output of our superconductive comparator at GHz speeds. Fig. 4 shows an experimental setup that could be used to acquire the digital data from the output of the comparator when it is clocked at a frequency of 1 GHz or more. An HP 16500C logic analysis system can be used as a fast shift register to acquire up to 64kb of digital data at 1 Gb/s. After a set of data are acquired, the data can be downloaded to a computer for fast Fourier transform (FFT) analysis. Low-frequency feedback with a bandwidth of a few Hz can be used to prevent the comparator from drifting from the desired operating point. Suppose that the comparator is operated such that  $P_{OUT} = 0.5$ . If the comparator clock is set to 1 GHz and 64k samples of data are acquired, then the total sample size,  $\Delta T$ , is 64  $\mu$ s. By performing an FFT on the acquired data set, the output spectrum can be observed with a frequency resolution of  $\Delta B = 1/\Delta T = 15.6$  kHz and over a bandwidth of 1 GHz. The 64kb data set must be sampled hundreds of times and the squares of the magnitudes of the FFTs must be averaged so that the average power spectrum can be obtained. If the comparator behaves ideally, we expect that this average noise power spectrum will be flat over the entire frequency range.

Now suppose that we repeat this experiment, but this time we apply a small sinusoidal input current at frequency  $\omega_0$ . We can find the minimum current amplitude,  $I_{3dB}$ , sufficient to

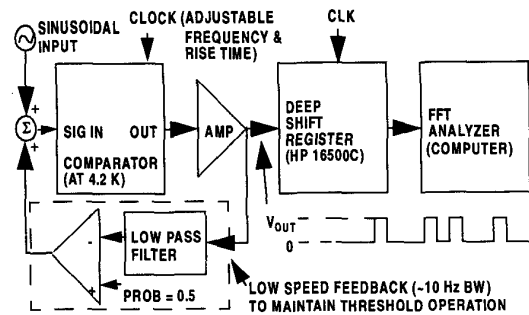


Fig. 4. Digital acquisition data collection scheme used to measure the energy sensitivity of the comparator and to inspect the magnitude of the noise floor up to half of the clock frequency,  $f_{CLK}$ . Low speed feedback is used to bias the comparator at its operating point, usually at  $P_{OUT} = 0.5$ .

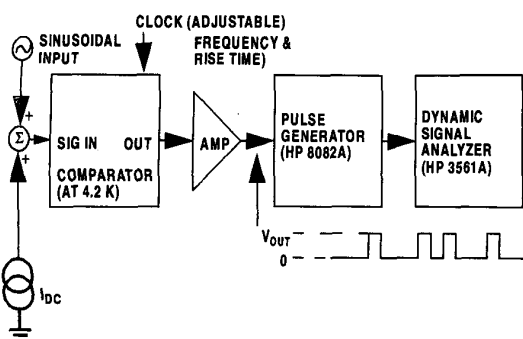


Fig. 5. Simplified energy sensitivity measurement experiment. An HP signal analyzer is used in place of a digital acquisition system and the computer shown in Fig. 4. The HP analyzer performs an FFT of the analog waveform.

allow the magnitude of the frequency bin corresponding to  $\omega_0$  to exceed the noise floor by 3 dB. This is the point where the signal equals the noise. We can now interpret eq. (7) in terms of this power spectral density experiment. The term  $\Delta E = [L(I_{3dB})^2]/2$  represents the potential energy fluctuations in the comparator due to the applied input flux at the frequency  $\omega_0$ . The term  $\Delta T = 1/\Delta B$  is the length of the FFT, or the time over which this sinusoidally applied energy  $\Delta E$  is to be resolved.

### III. EXPERIMENTAL MEASUREMENTS

We have not yet conducted experiments to measure the power spectral density and the energy sensitivity of a comparator when it is clocked at 1 GHz as was described in the last section (Fig. 4). Preliminary experiments, however, were conducted to measure the power spectral density and the energy sensitivity of a QFP comparator that was clocked at frequencies between 40 Hz and 40 MHz using the simplified experimental setup shown in Fig. 5. Note that we have omitted the low-frequency feedback loop shown in the more elaborate experimental setup of Fig. 4. Instead we have applied a manually controlled dc input to hold the comparator at the  $P_{OUT} = 0.5$  operating point. Also, we have replaced the digital FFT analysis tools comprising the HP 16500C logic analyzer (shift register) followed by a computer with a pulse generator (HP 8082A) followed by an analog FFT analyzer (HP 3561A). A clock is used to actuate the QFP comparator, to force it to "make a decision." That decision is represented by the direction that a current flows in its output inductor. This output inductor is the control line of a "readout" SQUID, which when biased by a slightly delayed "readout" clock (not shown), will either enter the voltage state or remain at zero volts, depending upon the sign of the inductor current ([6] for operation of the QFP and readout).

In the simplified experiment the pulse generator is used to generate large amplitude ( $\sim 1$  V) pulses every time the QFP readout generates a "1". These analog pulses are delivered to the input of an HP dynamic signal analyzer, which treats the

pulse stream as an analog signal. The analyzer band-pass filters the analog signal, resamples it using an A/D converter and performs an FFT on the sampled data so that the spectral content can be analyzed. The analyzer has the capability of acquiring and averaging the power spectra of a user-specified number of sampled waveforms, and hence an average power spectrum can be obtained.

This approach has the following advantages over the fully digitized approach: (1) the dynamic signal analyzer has the built-in capability of sampling the data and processing it with little setup effort, and (2) the noise spectrum can be measured with arbitrary resolution about a user-specified center frequency. We note that very long sequences of data are required (100s of megabits) in the fully digital experiment if sub-kHz resolution is desired, and this can be difficult to achieve. The disadvantage of using the simplified setup is that the output bits are processed as analog signals, so environmental noise, such as 60 Hz ripple, which couples into the output of the pulse generator, but which is not actually present in the input signal, can show up in the output power spectrum. Also, the analyzer has a front-end anti-aliasing band-pass filter with a bandwidth 100 kHz, preventing observation of the high-frequency noise floor.

Fig. 6 shows a typical output from the signal analyzer when a small ( $\sim 5$  nA) 31.0 kHz sinewave was applied to the input of the QFP, and the QFP was biased at its  $P_{OUT} = 0.5$  operating point. The QFP was clocked at 40 MHz. In this particular case, the analyzer was set to measure the average power spectrum (100 FFT averages) with a center frequency of 31.0 kHz with a resolution of 2.5 Hz. We see over the 1 kHz range of frequencies, the noise floor is flat except at the frequency bin at 31.0 kHz where the input sinusoid is applied. In Fig. 6 this frequency bin is 10 dB above the noise floor. We adjusted the amplitude of the applied input current (flux) so that the 31.0 kHz frequency bin was 3 dB above the noise floor. We could then establish the sensitivity of the comparator.

We also examined the spectrum from dc to 10 kHz in 25 Hz bin sizes, and we noted that the noise floor was flat, except at a few integer multiples of 60 Hz, where noise spikes were

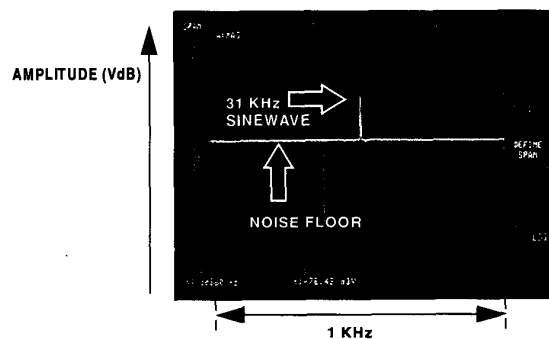


Fig. 6. Typical output of HP signal analyzer. A 31 kHz sinewave is applied to the input of the QFP comparator. The noise floor is flat except at the input frequency. The signal amplitude at which the signal is 3 dB above the noise floor can be measured, and the energy sensitivity can thus be computed.

observed. We suspect that the observed 60 Hz noise comes from pickup of line voltages into the output of the pulse generator and is not pickup which is present in the input waveform. One impetus for analyzing the output data in a purely digital format, rather than sampling the analog waveform, is that noise pickup in the output can be eliminated. We also measured the noise floor from dc to 100 kHz in 250 Hz bin sizes, and we again found the floor to be flat except at the 60 Hz multiples. When we measured the amplitude of the noise floor from dc to 10 Hz in 25 mHz steps, we observed that the floor began to rise below about 5 Hz. This low-frequency excess noise is due either to the excess noise that is found in the junctions of the comparator [12] or to low-frequency noise from our dc biasing apparatus. We also measured the magnitude of the noise floor, and we found it to be inversely proportional to the clock frequency from 40 Hz to 40 MHz as we expected. The margins in our readout circuit limited us to 40 MHz operation, and we are redesigning the readout circuit so that it will operate well above 1 GHz. As we approach 1 GHz operation and beyond, it is not clear whether the noise floor will remain white, and whether the noise floor will have a magnitude that is inversely proportional to the clock frequency as theory predicts. We suspect it will be necessary to more carefully shield the comparator from external noise to get agreement with theory.

Using the experimental setup shown in Fig. 5 we have computed the energy sensitivity of the QFP comparator at various clock frequencies with different clock rise times by measuring the slope of the gray zone  $dP/dI$  and by measuring the minimum detectable signal (refer to eq. (7)). Table I summarizes

TABLE I.

Energy sensitivity of QFP computed from eq. (7) by two methods: (1) from the slope of gray zone ( $dP/dI$ ) and (2) from the minimum detectable signal ( $I_{3dB}$ ).  $P_{OUT} = 0.5$  and the comparator's differential inductance was estimated to be 4.0 pH. Sensitivity is measured in units of Planck's constant ( $h = 6.02 \times 10^{-34}$  Js).

Freq.	Rise time	$dP/dI$	$I_{3dB}$	$S_E$ (gray zone)	$S_E$ ( $I_{3dB}$ )
MHz	s	$\mu A^{-1}$	nA	$h$	$h$
0.285	$10^{-6}$	0.267	5.5	82,000	41,000
0.285	$10^{-9}$	0.181	12.0	180,000	190,000
22.2	$10^{-8}$	0.224	1.2	1500	1900
40.0	$10^{-10}$	0.085	2.46	5800	8100

our experimental results. We have biased the comparator at its maximum gray-zone slope with  $P_{OUT} = 0.5$ . The comparator's differential input inductance was estimated to be 4.0 pH. In each case the bin width  $\Delta B$  was chosen to be 2.5 Hz, and we arbitrarily chose 31.0 kHz to be the frequency at which the  $I_{3dB}$  measurements were made. The reader should refer to [6] to understand the relationship between clock rise time and the gray-zone slope for the QFP comparator. We note for shorter clock rise times, the slope  $dP/dI$  is decreased, and hence  $S_E$  is

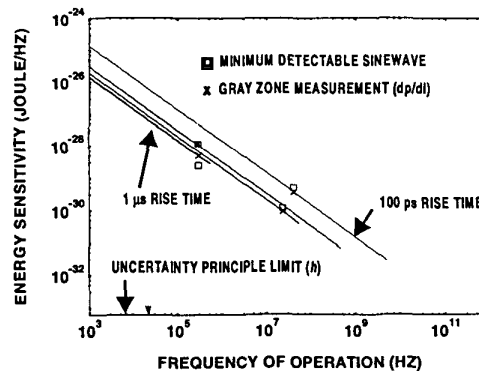


Fig. 7. Plot of energy sensitivity computed by two methods (Table I): (1) using method of minimum detectable signal (squares), and (2) using gray-zone ( $dP/dI$ ) method (crosses). Measurements were made at three different clock frequencies and with four different clock rise times. Lines represent projections of energy sensitivity for constant exciter rise times (constant values of  $dP/dI$ ) but for varied clock frequencies.

a larger number. Thus the comparator is less sensitive. The energy sensitivity calculations from the two measurement techniques are in agreement to within a factor of two. There were several potential sources of error, and further experiments will be required to understand why the two measurement techniques are not in closer agreement. Clearly resolving this issue is important for understanding a comparator's behavior. Fig. 7 shows a plot of the energy sensitivity results of Table I. Sensitivity values derived by the minimum-detectable-sinewave method are shown as squares, and those determined by gray-zone measurements are represented by crosses. The solid lines are projections of the energy sensitivity for constant exciter rise times (constant values of  $dP/dI$ ) but for varied clock frequencies. The right sides of the lines end at the highest possible clock frequency for the given exciter rise time. The value at which the energy sensitivity is best, when  $S_E$  is at a minimum, is shown on the graph as the uncertainty-principle limit ( $h$ ). This is the approximate limit at which the ultimate sensitivity has been reached. We believe with better comparator designs the slope  $dP/dI$  can be increased for a given clock rise time, and hence the sensitivities in Table I can be improved for the given clock speeds.

#### IV. PROPOSED CORRELATION EXPERIMENT

Our ultimate goal is to determine the highest clock frequency at which a comparator behaves ideally, which is the frequency at which its output power no longer spreads out uniformly across a bandwidth equal to the clock frequency. At this frequency a comparator may reach an energy sensitivity limit well before it reaches the ultimate uncertainty-principle limit ( $h$ ). To perform this ultimate test, it will be necessary to clock the comparator at 10s of GHz frequencies. At these

clock frequencies, it will be difficult to send the digital data to room temperature for FFT processing, even if the data is multiplexed and sent out on parallel channels. A simpler test to establish whether or not the comparator is behaving ideally is to measure the first term of the autocorrelation function. If the comparator behaves ideally, then its power spectrum should be white, and all non-zero terms of the autocorrelation function should be zero. Fig. 8 shows how a few on-chip logic gates could be used to measure the first term. The comparator is operated with  $P_{OUT} = 0.5$ . A delay element is added to the output of the comparator so that adjacent samples can be compared. The adjacent samples are routed pairwise into four logic blocks the first of which is used to determine if the bit pattern is "11". The second, third, and fourth logic blocks determine if the bit pattern is "01", "10", or "00" respectively. If adjacent samples are truly independent, as we would expect in the ideal comparator, then the outputs of each of the four logic blocks should generate a "1" with a 25% likelihood. An average-voltage measurement at the output of each of these blocks could be used to determine the relative probabilities of each sequence. These four voltage-levels should remain equal as the clock frequency is increased. At some frequency the comparator's settling time will be longer than the clock period, and hence adjacent bits will become correlated.

## V. CONCLUSIONS

We have proposed that the energy sensitivity of a comparator should be used as a benchmark of its performance. Studies of the gray zone are not sufficient to fully characterize the behavior of comparators operating at GHz clock frequencies. The entire power spectrum should be observed to ensure that the noise is white up to the clock frequency. We have proposed that the sensitivity should be computed in two different ways: by measuring the slope of the gray zone ( $dP/dI$ ) and by measuring the minimum detectable sinewave. Ideally, these two measurements should give identical results.

A set of sensitivity experiments was conducted on a QFP comparator from 40 Hz to 40 MHz, and good agreement between the two measurements of sensitivity was obtained. To observe the entire noise spectrum into the GHz range, we have

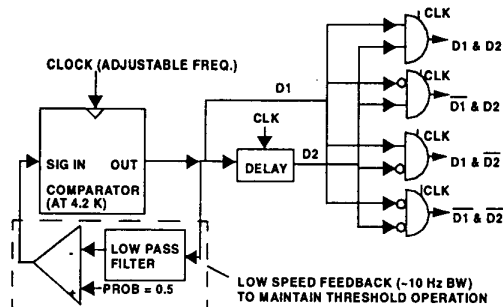


Fig. 8. Signal correlation experiment. First term of the autocorrelation function can be determined by measuring the frequency of the four different patterns: "00", "01", "10", and "11".

suggested an experiment to process the data digitally. For 10s of GHz clocking, we have also suggested an experiment to measure the first term of the autocorrelation function. We believe that there is much work to be done to confirm that comparators can be operated at their ultimate uncertainty-principle limits.

## REFERENCES

- [1] V. K. Seminov, Y. A. Polyakov, and D. Schneider, "Implementation of oversampling analog-to-digital converter based on RSFQ logic," extended abstracts of ISEC, pp. 41-43, 1997.
- [2] S. V. Rylov and R. P. Robertazzi, "Superconducting high-resolution A/D converter based on phase modulation and multichannel timing arbitration," IEEE Trans. Appl. Supercond., vol. 5, no. 2., pp. 2260-2263, June 1995.
- [3] D. L. Miller, J. X. Przybysz, A. H. Worsham, and A. Miklich, "Superconducting sigma-delta analog-to-digital converters," extended abstracts of ISEC, pp. 38-40, 1997.
- [4] V. K. Semenov, T. V. Fillipov, Y. A. Polonsky, and K. K. Likharev, "SFQ balanced comparators at a finite sampling rate," IEEE Trans. Appl. Supercond., vol. 7, no. 2, pp. 3617-3621, June 1997.
- [5] T. Fillipov, Y. A. Polyakov, V. K. Semenov, and K. K. Likharev, "Signal resolution of RSFQ comparators," IEEE Trans. Appl. Supercond., vol. 7, no. 2, pp. 2240-2243, June 1995.
- [6] H. Ko, and G. Lee, "Noise analysis of the quantum flux parametron," IEEE Trans. Appl. Supercond., vol. 2, no. 3, pp. 156-164, September 1992.
- [7] M. Radparvar and S.V. Rylov, "High sensitivity digital SQUID magnetometers," IEEE Trans. Appl. Supercond., vol. 7., no. 2, pp. 3682 - 3685, June 1997.
- [8] N. Fujimaki, H. Tamura, T. Imamura, and S. Hasuo, "A single-chip SQUID magnetometer," IEEE Trans. Appl. Supercond., vol. 35, no. 12, pp. 2412-2418, June 1988.
- [9] N. Fujimaki, K. Gotoh, T. Imamura, and S. Hasuo, "Thermal-noise-limited performance in single-chip superconducting quantum interference devices," J. Appl. Phys., vol. 7, no. 5, 15 June, 1992.
- [10] U. Faith, R. Hundhausen, T. Fregin, P. Gerigk and W. Eschner, "Experimental digital SQUID with integrated feedback circuit," IEEE Trans. Appl. Supercond., vol. 7, no. 2, pp. 2747-2751, June 1997.
- [11] N. Fujimaki, H. Tamura, T. Imamura, and S. Hasuo, "Thermal noise-limited sensitivity of the pulse-biased SQUID magnetometer," J. Appl. Phys., vol. 65, no. 4, 15 Feb, 1989.
- [12] C.T. Rogers and R. A. Buhrman, "Conductance fluctuations and low frequency noise in josephson junctions," IEEE Trans. Appl. Magn., vol. Mag-19, no. 3., pp. 453-457, May 1983.